



On 17-4PH stainless steel dental implant for premolar 4 in canine under compressive loading: effect of solid and octet metastructure

Bharat Kalia* , Rupinder Singh , Bahadur Singh Pabla , Gurwinder Singh 

Department of Mechanical Engineering, National Institute of Technical Teachers Training and Research, Chandigarh 160019, India

***Correspondence:** Bharat Kalia, Department of Mechanical Engineering, National Institute of Technical Teachers Training and Research, Chandigarh 160019, India. bharatkalia98@gmail.com

Academic Editor: John Hardy, Lancaster University, UK

Received: February 22, 2024 **Accepted:** August 8, 2024 **Published:** August 23, 2024

Cite this article: Kalia B, Singh R, Pabla BS, Singh G. On 17-4PH stainless steel dental implant for premolar 4 in canine under compressive loading: effect of solid and octet metastructure. *Explor BioMat-X*. 2024;1:202–14. <https://doi.org/10.37349/ebmx.2024.00015>

Abstract

Aim: The study aims to analyze the canine's implant behaviour under compressive loading [to be installed in a maxilla at a premolar 4 (PM4) location]. After simulation of various mechanical properties, the 17-4 precipitate hardened (PH) stainless steel (SS) prototypes were successfully 3D printed by powder bed fusion (PBF) process with solid and octet metastructure to reduce stress shielding.

Methods: The maxillary PM4 tooth of a male German shepherd dog was selected as the subject for the proposed study. As PM4 loading in canines is analogous to compressive loading conditions, finite element analysis (FEA) under compression was performed to compare simulated results of solid and octet metastructure specimens. Solid and octet meta structure-based compression samples were prepared per ASTM E9 standard using SolidWorks software. The octet metastructure was designed with node and connector diameters of 0.5 mm each on 3DXpert software. Further FEA analysis of designed compression samples was performed using Ansys Workbench by selecting 17-4PH SS material at loading conditions of 800 N and 5,000 N.

Results: The FEA results at the loading of 800 N show that maximum Von-Mises stress in the case of the solid and octet meta structure-based compression specimen was 10.029 MPa and 131.61 MPa, respectively. Further, the maximum Von-Mises strain for the solid and octet meta-structure-based specimens was 0.000049163 and 0.00067179, respectively. Similarly, deformation (in mm) for solid and octet truss lattice-based compression samples were 0.00075097 and 0.001451, respectively. The results observed at the loading condition of 5,000 N followed a pattern similar to that of 800 N loading conditions.

Conclusions: Octet metastructure-based compression sample showed encouraging potential for withstanding maximum compression loading applicable to canine (800 N) while lowering the impacts of stress shielding. The safety factor against failure (N) was 4.33 and 62.31 for the octet meta-structure and solid compression samples, respectively.



Keywords

Laser powder bed fusion, stress shielding, 17-4PH stainless steel, FEA analysis

Introduction

Additive manufacturing (AM) creates three-dimensional objects by layering two-dimensional cross-sections [1]. Metal AM is a rapidly growing global sector driven by advancements in fibre laser technology and lower equipment costs [2, 3]. Metal AM is used in industries like aerospace, automotive, and medical, as well as personal customization and powder waste management targeted to sustainable management goal (net zero target). AM technology has advantages in design, such as producing complicated shapes, being lightweight and efficient, allowing for personalized designs, and integrating components for better durability [4–6]. The AM technology can create complicated shapes beyond typical manufacturing methods like machining, casting, and metal forming, promotes innovation and increases design freedom.

Oral health is one of the essential concerns for the day-to-day activities performed by living organisms. Tooth are one of the vital organs needed by healthy animals to carry out various tasks [7]. Premolar (PM) teeth in dogs vary in size and number of roots. The PM4, sometimes called the carnassial tooth, is critical in canines because of its strong structure and unique use. Three strong roots set this tooth apart from the single- and double-rooted PMs that come before it. Dogs eat carnivorous foods, and the PM4 helps them do it efficiently by shearing and grinding their meal. As per reported literature on canines, when a dog or other canine is 6–8 months old, its 28 deciduous teeth change into 42 permanent teeth [8]. Eight teeth, however, are regarded as ST (strategic teeth). This group comprises four canine teeth, two M1 teeth in the mandible, and two PM4 teeth in the maxilla (Figure 1). These are classified as ST because of specific functions where some compressive and shearing forces are significant, such as shredding flesh or chewing food [9, 10].

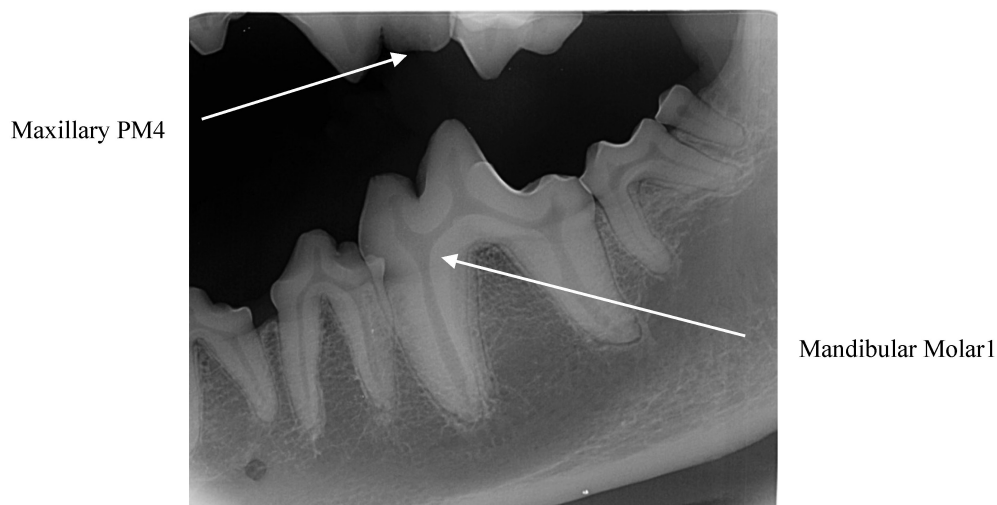


Figure 1. Maxillary PM4 (premolar-4) and mandibular M1 location

The first PM teeth in the upper (maxillary) and lower (mandibular) jaws are characterized by their petite, singular roots. Conversely, the maxillary PM4 presents a formidable structure with three distinct roots, while the remaining PMs exhibit a two-root configuration. Anatomically, the roots of each maxillary PM and M tooth are critical anatomical structures. Some animal teeth have three roots because animals have a larger biting force (between 800 and 850 N) than humans (between 80 and 90 N). This allows animals' teeth to withstand heavier loads [11].

A lattice structure is generally a porous structure created by arranging unit cells. The patterns determine the mechanical performance of the structure [12]. Lattice structures are more robust and lighter than non-lattice or solid structures and have a high strength-to-weight ratio due to their periodic arrangement of 3D unit cells [13, 14].

Strut-based lattices are ingeniously designed structures of linked struts and nodes that create a regular configuration of unit cells [15]. The lattice pattern propagates along the *X*, *Y*, and *Z* axes; these unit cells act as their basic building blocks [16]. A network of struts, thin load-bearing components joined at their intersections, usually makes up each unit cell [17]. The way in which these struts and nodes are arranged within the unit cell can be wildly varied, enabling designers to customize the mechanical properties of the lattice to meet particular needs [18]. They are beneficial in various applications, such as aeronautical, automotive, biomedical, and architectural engineering, since they may combine lightweight design with adaptable mechanical qualities [19]. The internal architecture, relative density, alloy material qualities, strut diameter and length, unit cell geometry, unit cell dimensions, and loading rate significantly impact lattice material [20, 21]. The configuration of struts, strut diameter/length, and unit cell orientation with angular aspects result in several lattice geometries with varying material properties. Therefore, the mechanical characteristics of lattice structures can be tuned for specific purposes, particularly in the biomedical field [22].

The most challenging aspect of bone implant implementation is the stress shielding effect due to an elastic modulus mismatch between the selected alloys for implant fabrication and the bone. Stress shielding may cause implant failure, which occurs when injured bone tissues with low elastic modulus are replaced with dense metallic alloys such as Ti-6Al-4V with high elastic modulus. Biometric structures, like lattice structures with low elastic modulus, are appropriate for resolving the mismatching problem. AM technique produces porous materials, which are critical for bone regeneration in biomedical implants. Porous structures further reduce the stress-shielding effect [23].

Porous and lattice structures are commonly employed in biomedical applications. Some studies have reported using biocompatible 17-4 precipitate hardened (PH) stainless steel (SS) for osseointegrated dental implant applications [24, 25]. AM technologies provide high porosity, which can improve osseointegration, facilitate bone ingrowth and regeneration, and provide stability across lattice structures [26].

Based on the provided literature, the “Web of Science (WoS)” database was analyzed to look at various studies conducted on the properties and analysis of dental implants made of SS using AM. Figure 2 shows the cluster of key phrases based on WoS data reported on dental implants. Thirty-four out of 818 terms met the requirement by choosing a minimum number of occurrences of the term “4”. Figure 2 displays the networking diagram as a bibliographic analysis based on the determined relevance score. Figure 3 shows the research gap as a network diagram based on bibliographic analysis.

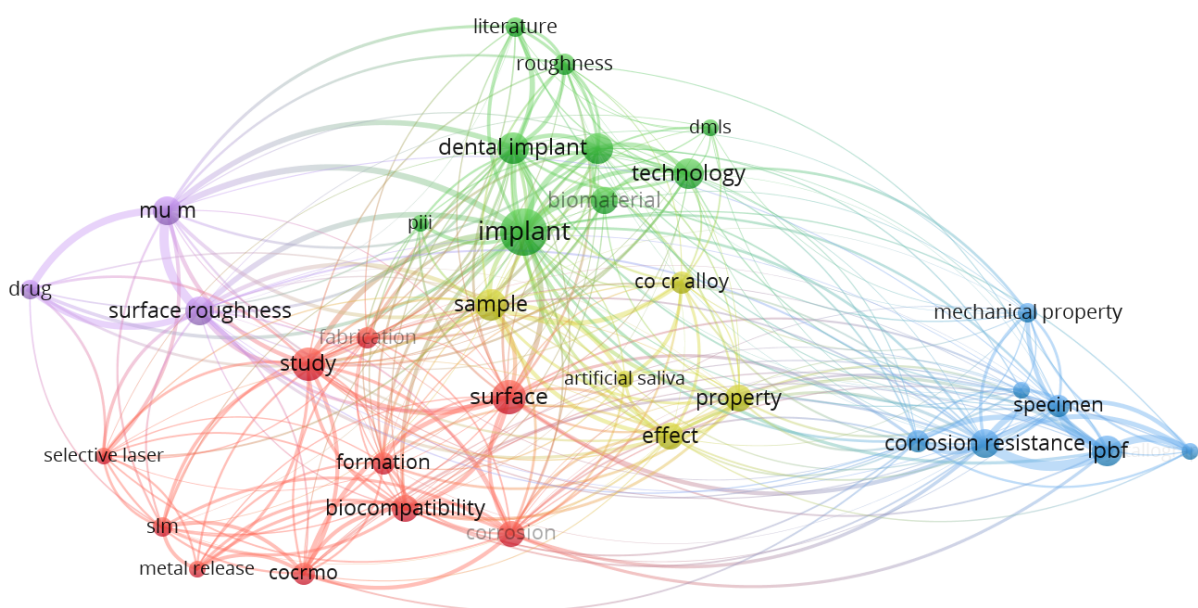


Figure 2. Bibliographic analyses for the keyword “stainless steel dental implant using additive manufacturing”

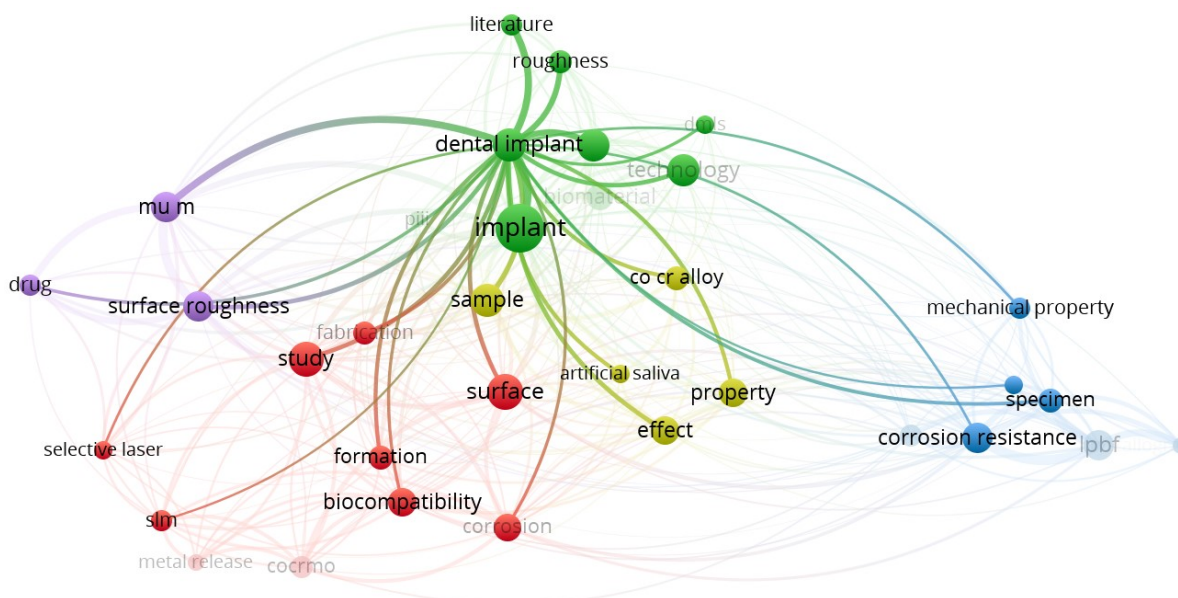


Figure 3. Gaps in previously reported literature related to lattice-based 17-4PH SS dental implants and DMLS

By investigating the compressive behaviour of solid and octet metastructure 17-4PH SS-based dental implants specifically for canine PM4, this study aims to provide new insights that can enhance/improve implant design and clinical outcomes in veterinary dentistry.

Dog tooth implants have emerged as a revolutionary remedy for various dental disorders in dogs. Dog tooth implants have become an attractive alternative for pet owners looking for long-term dental solutions. The carnassial tooth, or PM4, is essential to a dog's biting force and chewing mechanics. This tooth, positioned nearer the back of the jaw, is made especially for crushing and shearing food. Its structure, which is strong and has sharp cusps, makes it easier to crush and ground food or prey efficiently. Natural selection for mechanical efficiency in food processing is best illustrated by how the PM4 tooth in canines functions. This is similar to how compression testing assesses the toughness and durability of materials under stress. This tooth, which reflects the ideas used in compression testing to evaluate material qualities, demonstrates the significance of structural integrity and function by its capacity to sustain significant stresses when chewing.

Compression loading for canine dental implants is essential to their functional biomechanics. When a dog eats or bites, compression forces are applied to the implant, pushing it into the jawbone along its axis. This type of loading is crucial since a designed effective implant should predominantly experience compressive stresses that the bone can tolerate and aid in preserving implant stability. Compression loading promotes osseointegration, a process in which bone attaches to the implant, forming a strong attachment that resembles the natural tooth-root relation. This is especially crucial in the dynamic oral environment of pets, who frequently apply significant force while chewing. The purpose of designing and placing canine dental implants is to enhance compression loading while limiting other types of stress, like shear or lateral forces, that can be more harmful to implant-bone contact. The dental implant's durability and performance are greatly improved by obtaining a compression loading majority, giving a strong and dependable alternative for canine dental restorations. Combining lattice or metastructure innovation into canine dental implants provides various benefits that improve the overall success and efficiency of the implantation procedure. The lattice structure, comprised of titanium, improves osseointegration by stimulating bone growth into the implant. This results in a more secure and long-lasting link between an implant and the jawbone.

Furthermore, the lattice design ensures optimal weight distribution, minimizing stress on neighbouring bone and lowering the likelihood of problems. The porosity aspect of the lattice also promotes nutrition exchange, resulting in a healthier environment for bone tissue. Also, the lightweight yet strong properties of lattice/metastructure implants aid in surgical precision, making the surgery less intrusive and improving the dog's postoperative comfort.

This study evaluates and compares the functionality of implants designed to be installed in the canine femur's PM4 position under compressive loading circumstances. The study aims to determine if octet metastructure implants are strong and resilient enough to bear compressive stresses of up to 800 N in contrast with standard solid implants. Because of its well-known mechanical qualities and biocompatibility, 17-4PH SS has been selected for this comparative investigation. The work aims to assess the possible impact of octet metastructures in reducing the effects of stress shielding, a prevalent problem in orthopaedic implantation, by concentrating on the behaviour of implants under compressive loading.

Based on bibliographic analysis and literature review, it is revealed that several studies have been reported on using titanium and cobalt chromium-based alloys for dental implant applications using the DMLS process in the past decade. But hitherto, little has been reported on the effects of using different meta structures (solid vs octet) on the mechanical performance of 17-4PH SS-based dental implants under compressive loading.

Materials and methods

The maxillary PM4 tooth of a male German shepherd dog was selected as the subject for the study. This experiment is a simulation study based on an existing oral model of experimental animals (Ludhiana Lab, Guru Angad Dev Veterinary and Animal Sciences University, India) and does not involve any actual animals. Therefore, ethical approval from the animal experimentation ethics committee is not required. As PM4 loading in canines is analogous to compressive loading conditions, finite element analysis (FEA) under compression was performed to compare simulated results of solid and octet meta-structure specimens. The octet lattice structure was used, with node and connector diameters of 0.5 mm each. A thorough comparison of solid and lattice compression specimens is essential in dental implant applications for canine dogs, particularly in stress shielding. Both specimens were made of biocompatible 17-4PH SS, an alloy known for compatibility with biological conditions. The FEA analysis allowed a complete examination of the compression samples' mechanical behaviour, providing essential insights into stress distribution and potential regions of stress shielding. By comparing the performance of solid and lattice specimens, this study provides critical data for enhancing dental implant designs for canine applications. The methodology adopted for this study is shown in [Figure 4](#).

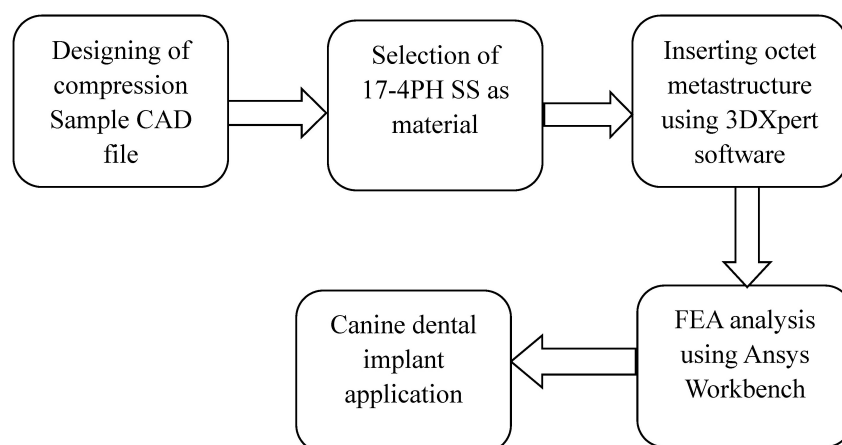


Figure 4. Adopted methodology for the study. FEA: finite element analysis; PH: precipitate hardened; SS: stainless steel

The use of octet lattice structures not only has the potential to minimize stress shielding but also opens up possibilities for improving the biocompatibility and functioning of dental implants in canine dogs. The CAD model of the octet metastructure-based compression sample ([Figure 5a](#)), octet unit cell ([Figure 5b](#)) and CAD model of the solid compression sample ([Figure 5c](#)) were designed using SolidWorks. This study is a significant advance in implant technology and increases the longevity and effectiveness of dental treatments in canine dogs.

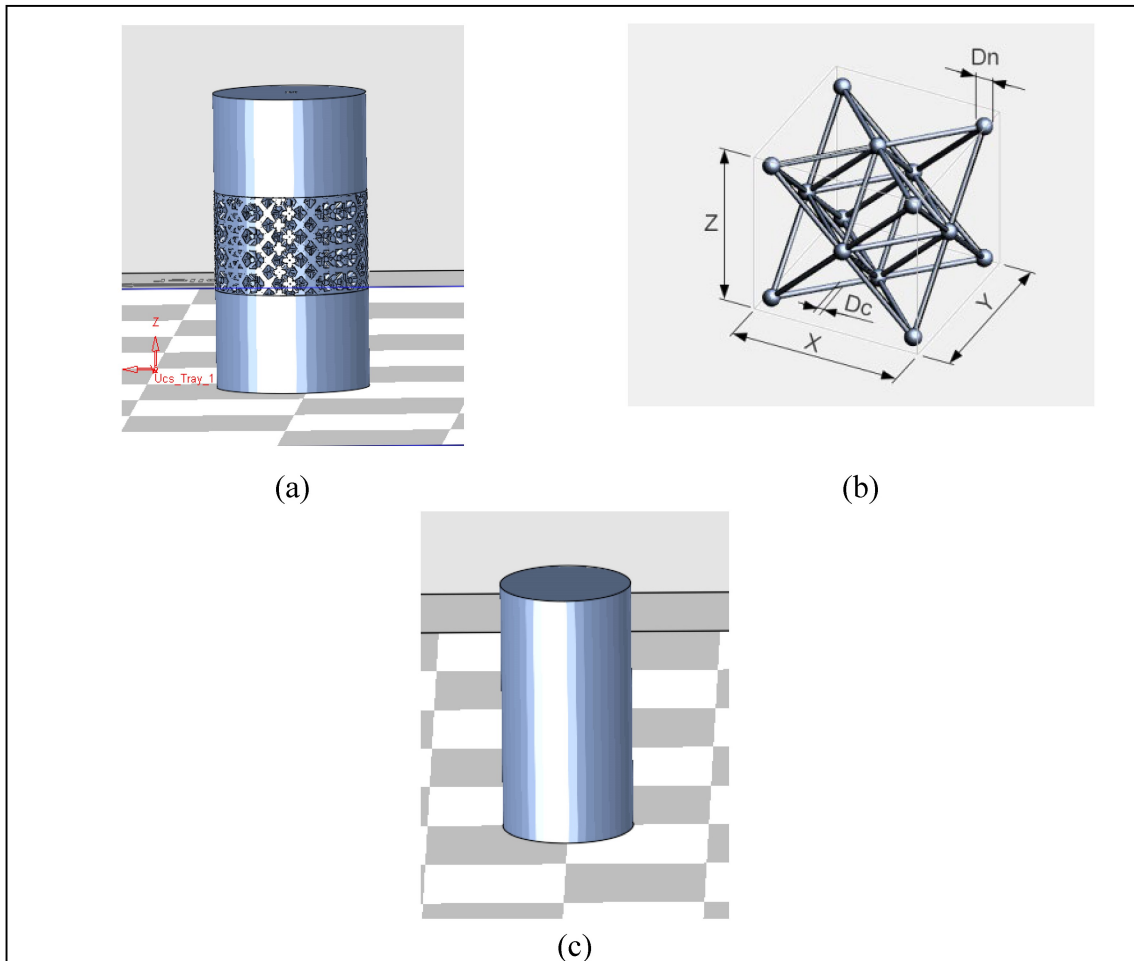


Figure 5. CAD model of octet metastructure-based compression sample (a), octet unit cell (b), solid compression sample (c)

Results

The simulation was run on solid and octet truss compression samples using Ansys Workbench (version R2-2022) software. Table 1 shows the deformation, elastic strain, and stress (Von-Mises failure criterion) for both samples of material 17-4PH SS under compressive loading. The FEA results are based on the Von-Mises criterion (800 N, 5,000 N applied load, cell type: tetrahedron). One end of the compression coupon was fixed to deliver the compressive load to the specimen. The literature revealed that 17-4PH SS build specimens with diamond cubic lattice on a pattern similar to octet metastructure give a yield strength of 570 MPa [27].

Table 1. FEA results of solid and octet metastructure-based compression specimen

Compression specimen	Load applied	Deformation (mm)	Elastic strain	Stress (σ_v) (MPa)	Yield strength (σ_y) at 0.2% of strain (MPa)	Safety factor against failure (N) = σ_y/σ_v
Solid	800 N	0.00075097 ± 0.0001	0.000049163 ± 0.00001	10.029 ± 1	625 ± 6 [25]	62.31 ± 6
Octet metastructure	800 N	0.001451 ± 0.001	0.00067179 ± 0.0001	131.61 ± 13	570 ± 5 [26]	4.33 ± 0.5
Solid	5,000 N	0.0046935 ± 0.001	0.00030727 ± 0.0001	62.682 ± 6	625 ± 6	9.97 ± 0.9
Octet metastructure	5,000 N	0.0090688 ± 0.001	0.002817 ± 0.001	545.57 ± 15	570 ± 5	1.04 ± 0.01

The FEA analysis of the specimen was done five times, and the average value was reported (average value ± SD). References [25] and [26] validate the observations. FEA: finite element analysis

As observed from [Table 1](#), the deformation value of the octet metastructure-based compression specimen is higher than the solid specimen at loading conditions of 800 N and 5,000 N. Since the solid specimen is more resilient to compression and has a consistent density than the lattice infill structure, it would typically undergo less deformation. The deformation value for the solid sample was less (0.00075097 mm) than the octet metastructure-based sample (0.001451 mm) under the 800 N compression loading condition. The results for the 5,000 N loading condition were also following a similar trend.

Von-Mises stress values were higher for the octet metastructure-based compression sample than solid compression samples under loading of 800 N and 5,000 N. The predicted σ_v value was 131.61 MPa for the octet metastructure sample compared to 10.029 MPa for the solid sample when subjected to an 800 N load. The trend observed in the results remains consistent even under 5,000 N loading. The Von-Mises stress value for the solid specimen would have a more uniform stress distribution than the one with octet lattice filling because the latter has interior structures or spaces. Both local and Von-Mises stresses may increase due to the stress concentration around the voids or lattice structure in the octet metastructure-based compression sample.

The equivalent elastic strain value for the octet metastructure compression sample was also higher (0.00067179) than the solid compression sample (0.000049163) while sustaining loads of 800 N. The 5,000 N loading yielded results following a similar observed trend. Since the octet lattice structure contains complicated deformation patterns, the Von-Mises elastic strain in the case of a lattice specimen would be more complex and non-uniform than in the case of a solid specimen. The octet lattice structure's elastic strain would likewise be dispersed unevenly, with more significant strains probably developing around the edges and intersections where stress concentrations are most important.

The literature revealed that 17-4PH SS build specimens with diamond cubic lattice on a pattern similar to octet metastructure give a yield strength of 570 MPa [28]. So, based on safety factor against failure (N) data, the octet metastructure-based specimen predicted a value of 4.33 for 800 N and 1.04 for 5,000 N compressive loading. The FEA simulation findings, as shown in [Figures 6 and 7](#), highlighted that the octet metastructure-based compression specimen offers significant reductions in stress shielding values and demonstrates comparable performance to that of the solid compression specimen.

So before fabricating compression coupons using a 3D printing process, pre-printing analysis of solid and octet metastructure-based compression samples was done on 3DXpert software by 3D systems, as shown in [Figure 8](#). The types of analysis performed were accumulated heat, accumulated stress, and boundary distortion stress. The values generated from the study were within range, leading to fabricating the compression coupon using a laser powder bed fusion process. The fabrication process was performed using a 3D metal printer (Model ProX DMP 200) by 3D Systems with a build platform of 140 × 140 × 100 mm and a 300 W fibre laser. 17-4PH SS powder with particle size 15–45 μm supplied by SRT Mumbai was used for fabrication. A high-precision laser melts together loose metal powder particles. The laser is pointed at the powder particles to create thin, successive horizontal layers selectively. The proportion of powder carried upwards by the feeding piston to the powder dispersed by the scraper is 3:1 [29].

The process parameters for fabricating the parts were Laser Power: 120 W, scan speed: 1,200 mm/s, hatch spacing: 50 μm , and layer thickness: 30 μm . Two types of compression samples with dimensions corresponding to the ASTM E9 standard were fabricated. The samples were printed successfully using the above printing parameters, as shown in [Figure 9](#).

The dental implant faces challenges in achieving both primary and secondary stability. Primary stability describes a dental implant's mechanical stability just after insertion. Primary stability is crucial because it impacts the healing process and establishes the first success of implant implantation. High primary stability minimizes implant micro-movements, which is necessary for osseointegration. Secondary stability is achieved through the biological process of osseointegration, where bone cells grow and adhere to the implant's surface. The long-term sustainability of the implant depends on secondary stability. It ensures the implant stays firmly fixed in the bone, allowing it to meet functional demands over time. The

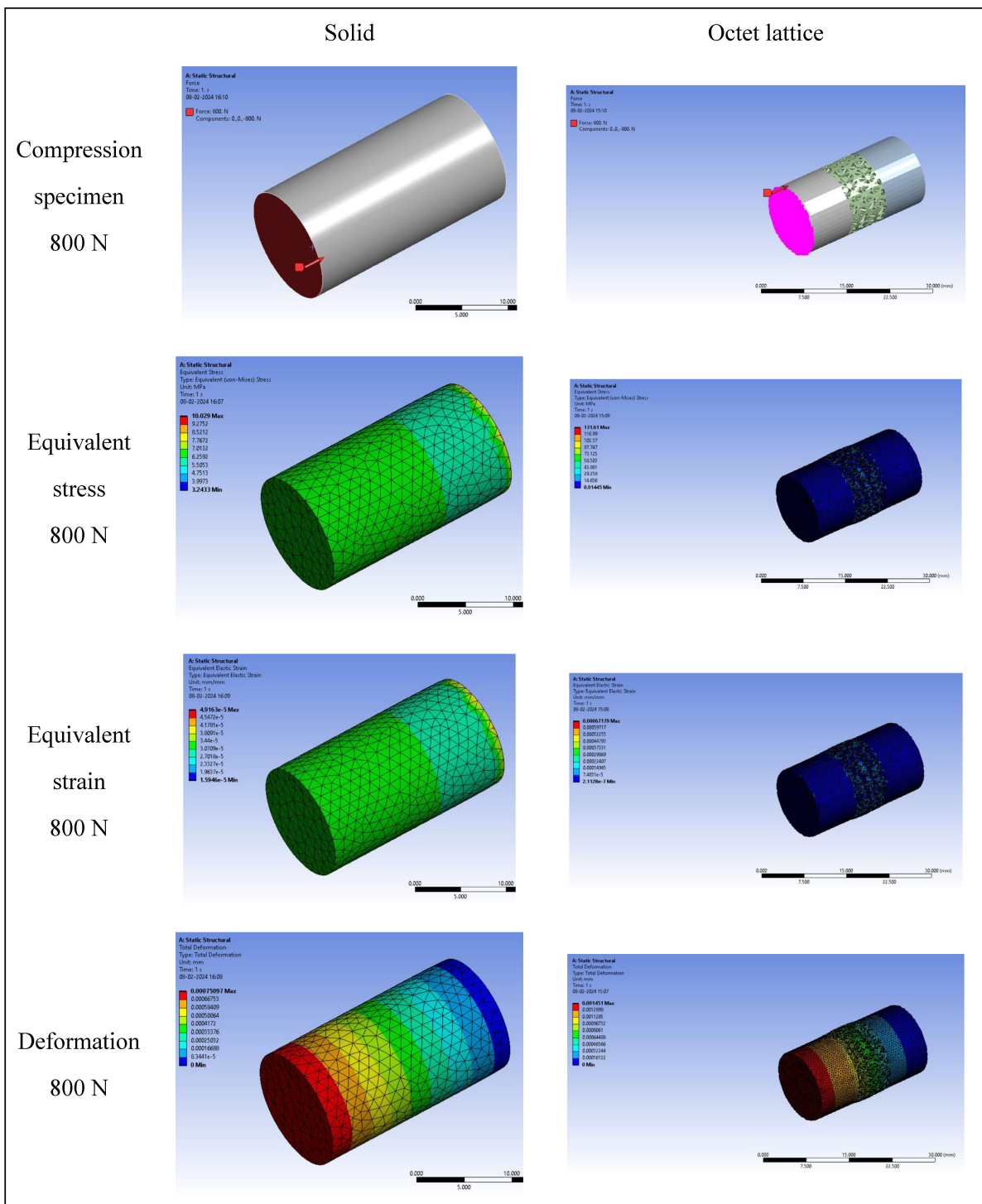


Figure 6. FEA result of compression specimen at 800 N loading. FEA: finite element analysis

current research is focused on addressing the primary stability of dental implants. The study related to the secondary stability of the implant will be reported in future work.

Further, future work might involve creating a Design of Experiments (DOE) to optimize printing parameters for improved quality and performance. The DOE seeks to determine the ideal set of parameters that produces printed samples with excellent mechanical qualities and dimensional accuracy by adjusting variables including laser power, scanning speed, and powder bed temperature. After that, experimental data regarding the compression samples will be produced using destructive testing methods. The resulting experimental data can be examined and contrasted with generated data from the FEA. The comparison analysis will thoroughly assess the simulation models' correctness and predictive power, confirming their effectiveness in forecasting the mechanical behaviour of printed components.

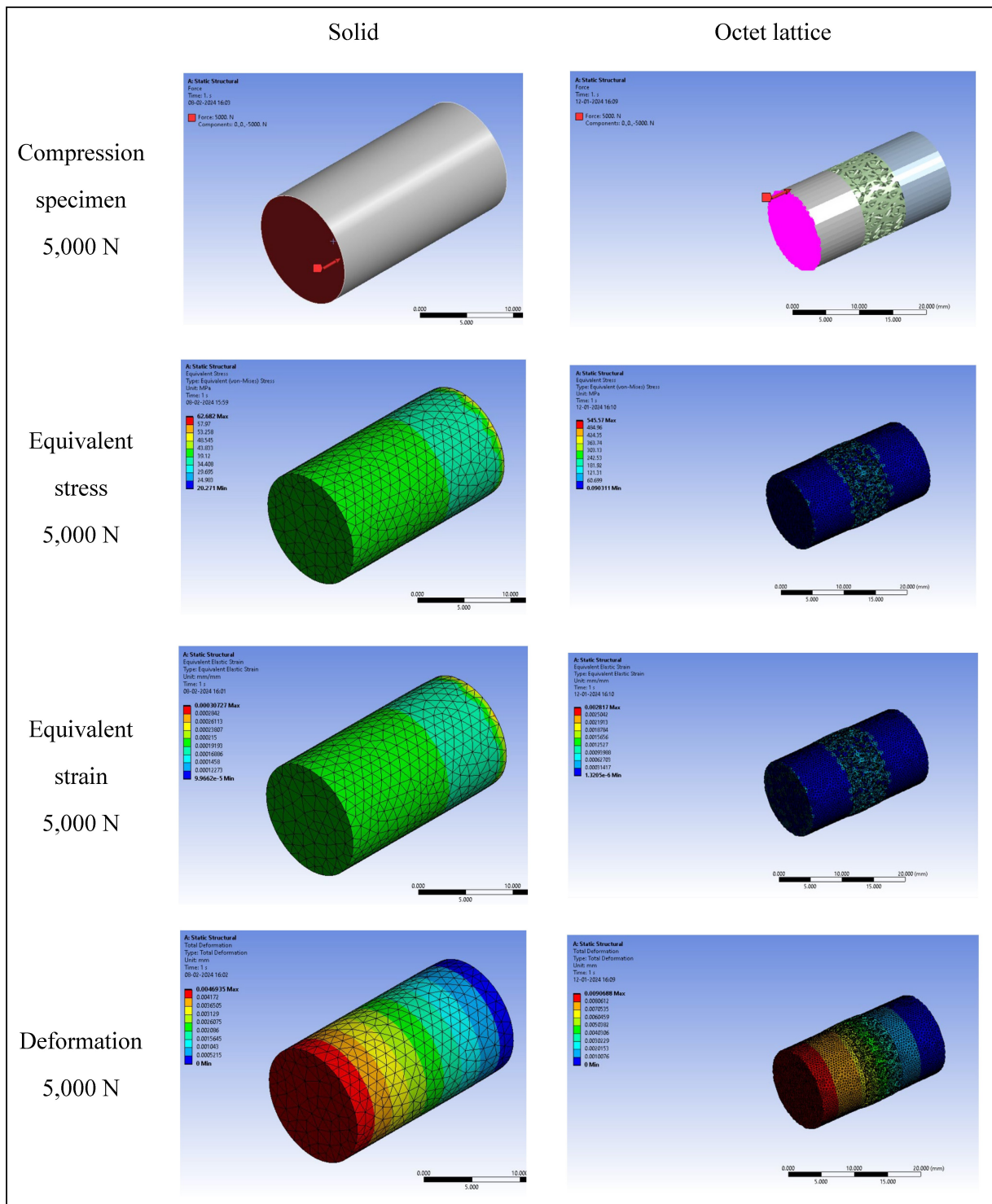


Figure 7. FEA result of compression specimen at 5,000 N loading. FEA: finite element analysis

Discussion

This work offers valuable insights into the feasibility of using octet metastructure-based standard compression specimens to address concerns about stress shielding and enhancing the long-term functionality of implants. The FEA findings showed that the octet metastructure-based compression specimen showed comparable safety and strength to the solid specimen under maximum compression loading conditions. Under 800 N compression loading conditions, the maximum safety factor against failure (N) for the solid compression sample was 62.31, while for the octet metastructure-based compression sample, it was 4.33. The octet metastructure shows improved load-bearing capacities compared to the solid

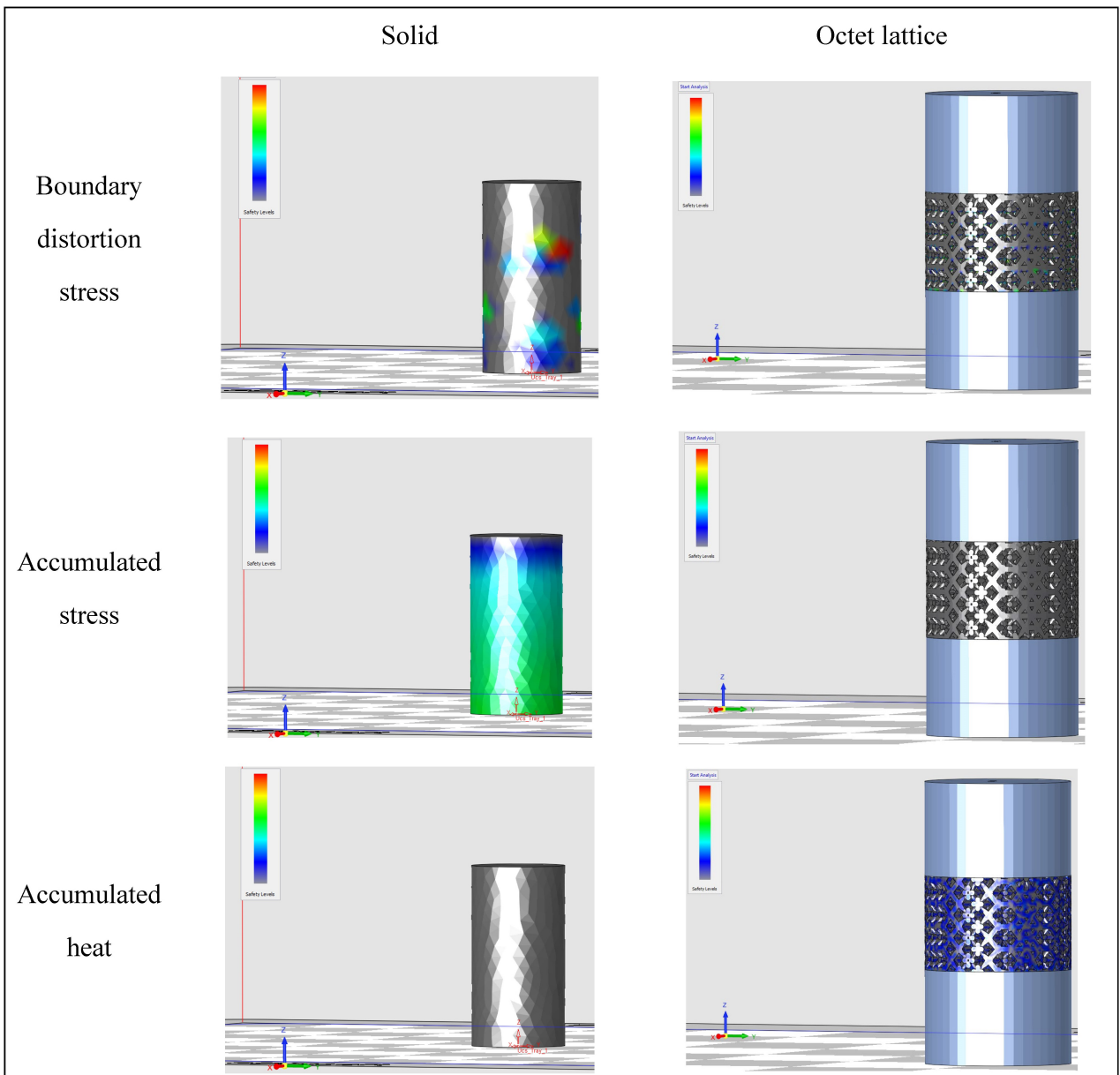


Figure 8. Pre-printing analysis using 3DXpert software



S. No.	Dimensions	Values (mm)
1	Total length	26
2	Diameter	13
3	Length of metastructure	8.66
4	Unit cell dimensions	$D_n = 0.5$ $D_c = 0.5$ $X = 1.5$ $Y = 1.5$ $Z = 2$

Figure 9. 3D printed specimen as per ASTM E9

specimen because of its unique geometric structure and mechanical characteristics. This demonstrates how metastructural designs can be used to improve the overall mechanical performance of materials in compression applications and mitigate the impacts of stress shielding. Future work might involve creating a DOE to optimize printing parameters for enhanced quality and performance. The DOE seeks to determine the ideal set of parameters that produces printed samples with excellent mechanical qualities and dimensional accuracy by adjusting variables including laser power, scanning speed and hatch distance.

Abbreviations

AM: additive manufacturing

DOE: Design of Experiments

FEA: finite element analysis

PH: precipitate hardened

PM4: premolar-4

SS: stainless steel

ST: strategic teeth

Declarations

Acknowledgments

The authors acknowledge the research support provided by the National Institute of Technical Teachers Training and Research Chandigarh and Prof. Ashwani Kumar from Guru Angad Dev Veterinary and Animal Sciences University Ludhiana.

Author contributions

BK: Investigations, Writing—original draft, Writing—review & editing. RS: Conceptualization. BSP: Supervisions. GS: Performed 3D analysis.

Conflicts of interest

Rupinder Singh who is the Guest Editor of Exploration of BioMat-X had no involvement in the decision-making or the review process of this manuscript. Other authors don't have any conflicts of interest/competing interests.

Ethical approval

This experiment is a simulation study based on an existing oral model of experimental animals (Ludhiana Lab, Guru Angad Dev Veterinary and Animal Sciences University, India) and does not involve any actual animals. Therefore, ethical approval from the animal experimentation ethics committee is not required.

Consent to participate

Not applicable.

Consent to publication

Not applicable.

Availability of data and materials

The authors declare that the data can be available on reasonable request.

Funding

The authors thank the Department of Science and Technology, National Institute of Technical Teachers Training and Research for funding under FIST Level-0 [SR/FST/College-/2020/997]. The funders had no role in study design, data collection and analysis, decision to publish, or preparation of the manuscript.

Copyright

© The Author(s) 2024.

References

1. Gao W, Zhang Y, Ramanujan D, Ramani K, Chen Y, Williams CB, et al. The status, challenges, and future of additive manufacturing in engineering. *Comput-Aided Des.* 2015;69:65–89. [DOI]
2. Conner BP, Manogharan GP, Martof AN, Rodomsky LM, Rodomsky CM, Jordan DC, et al. Making sense of 3-D printing: creating a map of additive manufacturing products and services. *Addit Manuf.* 2014; 1–4:64–76. [DOI]
3. Thompson MK, Moroni G, Vaneker T, Fadel G, Campbell RI, Gibson I, et al. Design for additive manufacturing: trends, opportunities, considerations, and constraints. *CIRP Ann.* 2016;65:737–60. [DOI]
4. Yang L, Hsu K, Baughman B, Godfrey D, Medina F, Menon M, et al. *Additive Manufacturing of Metals: The Technology, Materials, Design and Production.* Cham: Springer; 2017. [DOI]
5. Kang D, Park S, Son Y, Yeon S, Kim SH, Kim I. Multi-lattice inner structures for high-strength and lightweight in metal selective laser melting process. *Mater Des.* 2019;175:107786. [DOI]
6. Milewski JO. Additive manufacturing metal, the art of the possible. In: *Additive Manufacturing of Metals.* Cham: Springer; 2017. pp. 7–33. [DOI]
7. Coffman C, Visser C, Soukup J, Peak M. Crowns and prosthodontics. In: Lobprise HB, Dodd JR, editors. *Wiggs's Veterinary Dentistry: Principles and Practice.* John Wiley & Sons; 2019. pp. 387–410. [DOI]
8. Petruka A. Small Animal Dental, Oral & Maxillofacial Disease: A Color Handbook. *Can Vet J.* 2020;61: 188. [PMC]
9. Lemmons M, Beebe D. Oral anatomy and physiology. In: Lobprise HB, Dodd JR, editors. *Wiggs's Veterinary Dentistry: Principles and Practice.* John Wiley & Sons; 2019. pp. 1–24. [DOI]
10. Pradhan SR, Singh R, Banwait SS. On 3D printing of dental crowns with direct metal laser sintering for canine. *J Mech Sci Technol.* 2022;36:4197–203. [DOI]
11. Singh R, Das A, Anand A. On 3D printing of customized multi-root dental implants for the strategic tooth of canine by direct metal laser sintering. *Rapid Prototyping J.* 2023;29:447–59. [DOI]
12. Wahab RDA, Azman AH. Additive manufacturing for repair and restoration in remanufacturing: an overview from object design and systems perspectives. *Processes.* 2019;7:802. [DOI]
13. Vasiliev VV, Barynin VA, Razing AF. Anisogrid composite lattice structures - development and aerospace applications. *Compos Struct.* 2012;94:1117–27. [DOI]
14. Seharang A, Azman AH, Abdullah S. A review on integration of lightweight gradient lattice structures in additive manufacturing parts. *Adv Mech Eng.* 2020;12:1687814020916951. [DOI]
15. Brooks WC, Sutcliffe WC, Cantwell P, Fox J, Todd, Mines R. Rapid Design and Manufacture of Ultralight Cellular Materials. In: *Solid Freeform Fabrication Symposium. SFF Symposium 2005: Proceedings of the 16th Solid Freeform Fabrication Symposium; 2005 Aug 1–3; Austin, US.* pp. 231–41.
16. Gümrük R, Mines RAW, Karadeniz S. Static mechanical behaviours of stainless steel micro-lattice structures under different loading conditions. *Mater Sci Eng A.* 2013;586:392–406. [DOI]
17. Deshpande VS, Fleck NA, Ashby MF. Effective Properties of the octet-truss lattice material. *J Mech Phys Solids.* 2001;49:1747–69. [DOI]
18. Helou M, Kara S. Design, analysis and manufacturing of lattice structures: an overview. *Int J Comput Integr Manuf.* 2018;31:243–61. [DOI]
19. Maloney KJ, Fink KD, Schaedler TA, Kolodziejska JA, Jacobsen AJ, Roper CS. Multifunctional heat exchangers derived from three-dimensional micro-lattice structures. *Int J Heat Mass Tran.* 2012;55: 2486–93. [DOI]

20. Dantas ACS, Scalabrin DH, De Farias R, Barbosa AA, Ferraz AV, Wirth C. Design of Highly Porous Hydroxyapatite Scaffolds by Conversion of 3D Printed Gypsum Structures – A Comparison Study. *Proc CIRP*. 2016;49:55–60. [DOI]
21. Yoo DJ. Computer-aided porous scaffold design for tissue engineering using triply periodic minimal surfaces. *Int J Precis Eng Manuf*. 2011;12:61–71. [DOI]
22. Abdulhadi HS, Mian A. Effect of strut length and orientation on elastic mechanical response of modified body-centered cubic lattice structures. *Proc Inst Mech Eng Part L*. 2019;233:2219–33. [DOI]
23. Li Y, Yang C, Zhao H, Qu S, Li X, Li Y. New Developments of Ti-Based Alloys for Biomedical Applications. *Materials (Basel)*. 2014;7:1709–800. [DOI] [PubMed] [PMC]
24. Mutlu I, Oktay E. Characterization of 17-4 PH stainless steel foam for biomedical applications in simulated body fluid and artificial saliva environments. *Mater Sci Eng C Mater Biol Appl*. 2013;33:1125–31. [DOI] [PubMed]
25. Mutlu I, Oktay E. Influence of fluoride content of artificial saliva on metal release from 17-4 PH stainless steel foam for dental implant applications. *J Mater Sci Technol*. 2013;29:582–8. [DOI]
26. Gürkan D, Sağbaş B. Additively manufactured Ti6Al4V lattice structures for biomedical applications. *Int J 3D Print Technol Digital Ind*. 2021;5:155–63. [DOI]
27. Yadollahi A, Shamsaei N, Thompson SM, Elwany A, Bian L. Mechanical and microstructural properties of selective laser melted 17-4 PH stainless steel. In: *International Mechanical Engineering Congress and Exposition. IMECE 2015: Proceedings of the ASME 2015 International Mechanical Engineering Congress and Exposition; 2015 Nov 13–19; Houston, US. ASME; 2015*. [DOI]
28. Sabooni S, Chabok A, Feng SC, Blaauw H, Pijper TC, Yang HJ, et al. Laser powder bed fusion of 17–4 PH stainless steel: A comparative study on the effect of heat treatment on the microstructure evolution and mechanical properties. *Addit Manuf*. 2021;46:102176. [DOI]
29. Kalia B, Singh R, Pabla BS, Dureja M. On Direct Metal Laser Sintering of Functionally Graded Material with Virgin and Mixed Powder. *Arabian J Sci Eng*. 2024;49:11857–70. [DOI]